Chinese Journal of Polymer Science Vol. 33, No. 6, (2015), 899–907

Chinese Journal of Polymer Science

Asymmetric Ni/PVC Films for High-performance Electromagnetic Interference Shielding*

Yang Zhang**, Xiao-xia Fang and Bian-ying Wen**
Department of Material Science and Engineering, Beijing Technology and Business University, Beijing 100048, China

Abstract A novel asymmetric Ni/PVC film has been developed by solution casting method. The structure, electrical conductivity, electromagnetic interference (EMI) shielding, and impact resistance were investigated. The results showed that the Ni particles were asymmetrically distributed along the thickness direction in the film. The top surface resistivity increased with film thickness, while the bottom surface exhibited the different trend. EMI shielding effectiveness (SE) depended on formation of closed packed conductive Ni network, which was influenced by both Ni content and film thickness. A linear relationship was observed between EMI SE and film thickness. The films with lower Ni content showed the faster increasing rate of EMI SE with film thickness. Some of the films show appreciably high EMI SE (> 40 dB), indicating the promising application in EMI shielding field. Moreover, the films exhibit different impact performance under different impacting directions. All the experimental facts demonstrate that the asymmetric structure endows the film achieving high-performance EMI shielding function.

Keywords: Asymmetric structure; Electrical conductivity; Electromagnetic interference shielding.

INTRODUCTION

With the exponential increase in development of commercial, aerospace, military and scientific electronic devices in modern society, electromagnetic radiation is becoming the fourth public pollution after the air, water and noise ones[1]. The unwanted electromagnetic radiations and interference emitted from nearby instruments can degrade reliability, lifetime and efficiency of electrical devices[2]. Electromagnetic interference (EMI) shielding materials are essential to protect the sensitive circuits from unwanted electromagnetic radiations because they can reduce or suppress the electromagnetic noise.

Compared with conventional metal-based EMI shielding materials, conductive fillers/polymer composites with effective EMI shielding performance are more attractive due to their cost effectiveness, flexibility, great design freedom, and processing advantages. In general, conductive fillers, such as metal particles[3, 4], metal flake[5], carbon nanofiber[6, 7], carbon nanotube (CNT)[8], and graphene[9] are often used to embed in polymer matrices to enhance the conductivity and EMI shielding property of the composites. Among various polymer-based EMI shielding composites, films or sheets, which hold unique planar properties with remarkable combination advantages in mechanical flexibility and easy processing, have attracted more attention[10–13]. But in

* This work was financially supported by the National Natural Science Foundation of China (Nos. 21274007 and 51021064), the Project of Science and Technology Innovation Platform of Beijing Municipal Education Commission (No. PXM2012-014213-000025), the Tribology Science Fund of State Key Laboratory of Tribology (No. SKLTKF12A10) and Beijing Technology and Business University Natural Science Youth Foundation (No. QNJJ2012-29).
** Corresponding authors: Yang Zhang (张扬), E-mail: zhyang@iccas.ac.cn
Bian-ying Wen (温变英), E-mail: wenbianying@tsinghua.org.cn
Received October 21, 2014; Revised December 10, 2014; Accepted December 10, 2014
doi: 10.1007/s10118-015-1641-z

order to achieve the same shielding effectiveness (SE) as metal materials, a large conductive filler volume fraction and/or sufficiently large film thickness were usually required. These drawbacks increase the composite cost and thus limit its commercial use. Therefore, there is a growing requirement to develop comparatively thin films with high shielding performance, which would provide promising applications in EMI shielding field especially in areas of automobiles, aerospace, and fast-growing next-generation flexible electronics such as wearable devices. A novel approach to achieve this purpose is to produce films with particular structure.

Recently, lots of attentions paid on the asymmetric polymeric composites[14–17]. The internal structure or components are varied, usually along the thickness direction, in the composites. The properties such as electrical, elasticity modulus, heat conductivity, *etc*. are graded spatially, showing unique potential applications in many cutting-edge fields[18–20]. Hu and coworkers[10] have fabricated asymmetric sandwich structures for EMI shielding investigation by layer-by-layer method. Three main steps were employed in this fabricating process. A silver nanowire/PEO solution was first prepared on PET substrates by Meyer rods, and then put in an oven to remove PEO. After hot pressed, a poly(ethersulfone) (PES) wet film was used to coat the silver nanowire layer by a drawn-down rod-coating technique. Finally, a PET/silver nanowire/PES three-layered sandwich structure film was formed. The resulting hybrid composite structures showed high-efficiency EMI SE about 38 dB. Song and coworkers[11] fabricated wax|PVA| multilayer graphene nanosheets-EVA film|PVA| wax films in the sandwich structures. The optimized SE could be up to 27 dB with 60 vol% filler loadings at 0.35 mm film thicknesses. Compared with the elaborate layer-by-layer method, another facile strategy to fabricate asymmetric polymeric composites is by a one-step process using the casting strategy. Wu and coworkers[14] developed permittivity asymmetric composites by casting the CNTs/cyanate ester mixture into a mold for gravity sedimentation. The CNTs were gradient distributed in cyanate ester matrix along the thickness direction. This asymmetric composite had high permittivity and extremely low dielectric loss factor compared to the uniform composite. However, little work has been reported on the relationship between the electrical, EMI shielding, mechanical capabilities and the asymmetric film or on the underlying mechanisms.

In addition, compared to thick shielding materials (at millimeter scale), it is a challenge to fabricate EMI shielding film with much small thickness (less than one millimeter scale). Solution casting is a well-developed technique for fabricating thin films. The structure of the resulting film may be different from expectations derived from the original composition of the casting solution. As a consequence, we are intrigued by the opportunities to create high-efficiency EMI thin films with unique structure *via* a controllable route. Moreover, the possibility of multiple compartments offers the potential for low-temperature thermistor applications[21] or as an electric self-regulating heater[22].

In this work, we present a facile way to prepare asymmetric films at ambient conditions. Ni particles were chosen as the conductive filler due to their cheap price, ferromagnetic nature and a relatively high magnetic permeability[23, 24]. Thin films were prepared by means of solution casting method. The structure, electrical conductivity, EMI shielding, and impact resistance are intensively investigated. The results revealed that this asymmetric film was indeed a novel promising candidate for application in EMI shielding industry.

EXPERIMENTAL

Materials

Commercial Ni particles (1.5 μm) with a purity of 99.7 wt% were supplied by Wuxi ShunDa Metal Powder Co., Ltd.. Polyvinyl chloride (PVC, SG-2) was purchased from Tianjin Letai Chemical Co.. Tetrahydrofuran (THF, AR) was manufactured by Beijing Chemical. Co. Dioctyl phthalate (DOP) plasticizer was obtained from QiLu Chemical Co.. All the above materials were used as received.

Fabrication of Ni/PVC Films

Ni/PVC films with different thickness were prepared in the following steps. Firstly, PVC was dissolved in THF to form a 0.12 g/mL solution by using a mechanical stirrer. Secondly, DOP (W_{DOP}:W_{PVC} = 20:100) and the required amount of Ni particles were added into the above solution. The solutions were homogenized under

vigorous stirring for over 8 h. After that, the casting solution was immediately poured into an evaporating dish. Then, the evaporating dish was placed horizontally for 16 h at room temperature to allow the THF to evaporate. Finally, the Ni/PVC film was obtained from the evaporating dish and further dried in a vacuum oven at 30 °C for more than 6 h to remove the remaining solvents from the films. By varied the volume of the casting solution poured into the evaporating dish, a serious of different film thickness ranged from 0.17 mm to 0.45 mm was obtained. The films were cut to desired sizes for various measurements. During fabricating process, the surface which is corresponding to the evaporating dish is termed as the bottom surface and the air interface side is termed as the top surface.

Characterization

The surface morphologies of Ni/PVC films were observed by scanning electron microscopy (SEM, FEI, Quanta FEG 250). Cross-sections of the films were cryo-fractured from liquid nitrogen. All the samples were sputter-coated with gold before imaging. Surface resistivity measurements were conducted using two different instruments. For films with surface resistivity above 10^6 ohm, an EST-121 high resistance meter (Beijing Municipal Institute of Labor Protection, China) was used according to ASTM D257. For films with surface resistivity lower than 10^6 ohm/ square, a four-point probes resistivity measurement system (Four Probes Tech, RTS-9, Guangzhou, China) was performed. Data of surface resistivity were taken as averages of at least five measurements. Based on ASTM D4935-10, EMI shielding measurements were performed on an Agilent E5071C vector network analyzer (VNA) using 201-point averaging in the frequency range of 60 MHz–1.5 GHz. Impact resistance was performed using a plastic film pendulum impact tester (Changchun ChuangYuan Test Facility Co., JM-3, Changchun, China) with a 12.7 mm diameter hemispherical head, according to ASTM D3420-2008a standard. The capacity of the pendulum was 3 J. The results of impact resistance were averaged over ten measurements.

RESULTS AND DISCUSSION

Morphological Characterization

Figure 1 shows the representative SEM micrographs of surface and cross-sectional morphologies for Ni/PVC films with 8 vol% Ni particles (termed as 8 vol% Ni/PVC film). From Figs. 1(a) and 1(g), interestingly, it is clearly observed that the top and bottom surfaces of Ni/PVC film with the thickness of 0.17 mm exhibit different morphologies. High-resolution SEM micrographs in inset of Figs. 1(a) and 1(g) reveal the structural details, showing more Ni particles embedded in PVC matrix for the bottom surface than that for the top one. The surface morphologies of relatively thick films, such as 0.32 mm (c.f., Figs. 1b and 1h) and 0.44 mm (c.f., Figs. 1c and 1i), represent the similar structures as those of the 0.17 mm ones. A careful examination of surface morphological results indicate that the content of Ni particles in the top surface was decreased with the film thickness (c.f., Figs. 1a, 1b and 1c). But the bottom surface shows a different tendency. The content of Ni particles was increased for the bottom surface with the film thickness, as shown in Figs. 1(g), 1(h) and 1(i). In order to clarify the distribution of Ni particles in the films, the cross sectional sample of 8 vol% Ni/PVC films with thickness of 0.32 mm was observed. Different from the conductive fillers homogeneously distributed in traditional conductive filler/polymer composites, the cross-sectional morphology clearly demonstrates that the concentration of Ni particles increased from top surface to bottom surface along the thickness direction, as shown in Figs. 1(d), 1(e) and 1(f). There are few Ni particles seen in the upper part of the films (c.f., Fig. 1e), while a large number of Ni particles are observed in the lower part (c.f., Fig. 1f). More Ni networks are formed within an insulating PVC background in the lower part than those in the upper part. All the Ni/PVC films in this study showed the similar structure.

The above results clearly indicate that the Ni particles were asymmetrically distributed along the film thickness direction. We suggest this interesting asymmetrical distribution of Ni particles is arisen primarily from sedimentation during solution casting process, because the density of Ni particles is much larger than that of PVC. In other words, during the solvent evaporating process, the Ni particles in the system sink to the lower part

of casting films due to gravity, resulting in less Ni particles dispersed in the upper part (as shown in Fig. 1e) and the enrichment of Ni particles (as shown in Fig. 1f) in the lower part of the film. Under the given conditions, in order to obtain thicker films with the same Ni volume fraction, a larger amount of casting solution is required. This will lengthen the solvent evaporation time, resulting in more sedimentation time for Ni particles. There are indeed more Ni particles in solution with higher casting solution volume, but these Ni particles have a longer time to sediment. The sedimentation time is one of the key aspects for guaranteeing the distribution of Ni particles in the film. In consequence, less Ni particles accumulate at the top surface, whereas more Ni particles sediment toward the evaporating dish with film thickness increased. In briefly, Ni particles asymmetrically distributed along the thickness direction can be attributed to relatively heavy weight of Ni particles that drew them to the bottom of films by gravity. With increasing the film thickness, the content of Ni particles became lower in the top surface and Ni particles exhibited a denser distribution in the bottom surface. Based on our results, gravity sedimentation is the major factor for the formation of this asymmetric Ni/PVC films.

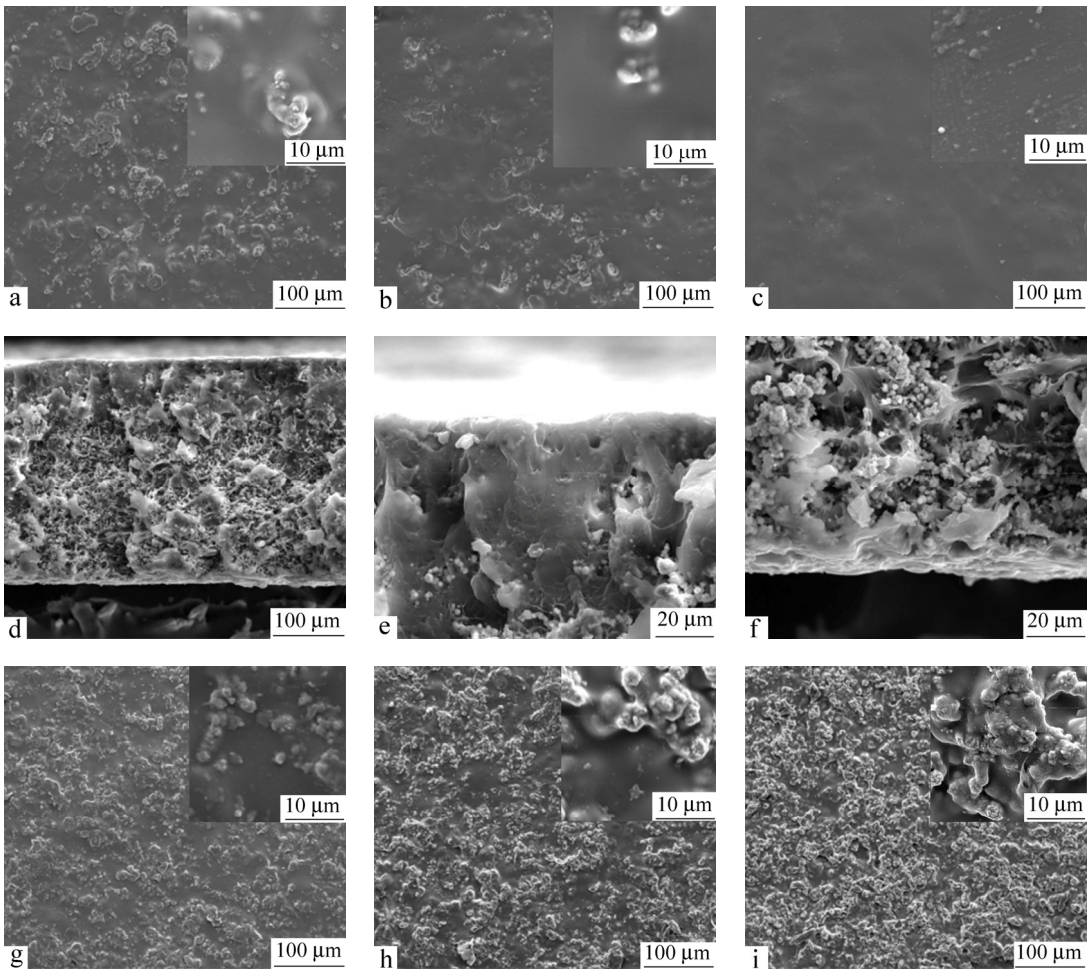

Fig. 1 SEM images of top surface of 8 vol% Ni/PVC films with thickness of (a) 0.17 mm, (b) 0.32 mm, (c) 0.44 mm; Cross sectional images of (d, e) upper part, (f) lower part of Ni/PVC film with thickness of 0.32 mm; Images of bottom surface of 8 vol% Ni/PVC film with thickness of (g) 0.17 mm, (h) 0.32 mm and (i) 0.44 mm (The insets of (a)–(c) and (g)–(i) correspond to higher magnification SEM images.)

Electrical Conductivity

The volume resistivity was usually adopted to evaluate electrical conductivity properties of traditional conductive filler/polymer composites due to conductive fillers homogeneously distributed in polymer matrix. But in the present work, the content of Ni particles varies along the film thickness direction as mentioned above, so the surface resistivity testing was chosen instead of volume resistivity measurement in this study. Figure 2 illustrates the surface resistivity as a function of film thickness. From Fig. 2, it is obvious that the surface resistivity of Ni/PVC films has great dependence on the thickness, especially for 8 vol% Ni/PVC films. The top surface resistivity increases with film thickness as evident from Fig. 2(a). An increase in surface resistivity from 1.48×10^9 Ω to 1.26×10^{10} Ω was observed with the thickness increased from 0.25 mm to 0.44 mm of 8 vol% Ni/PVC films.

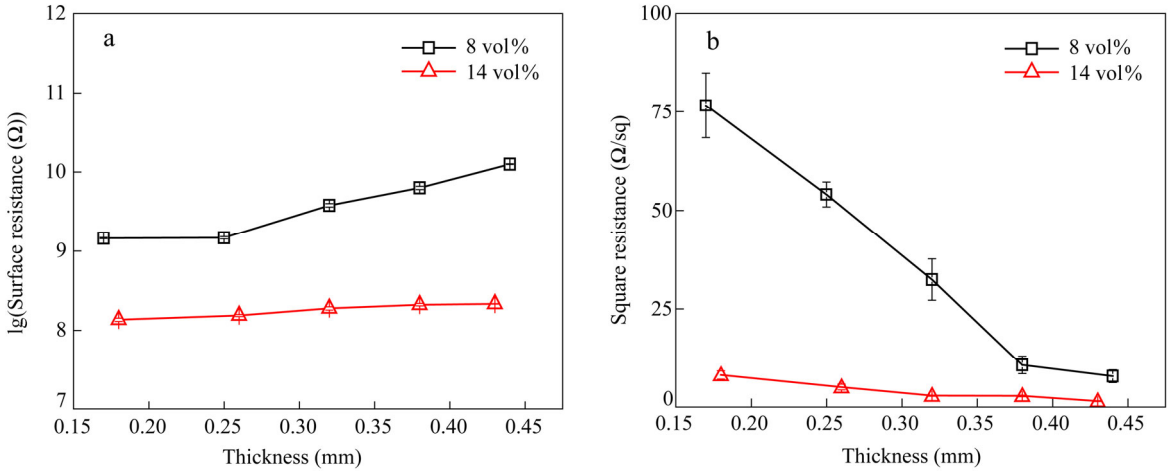

Fig. 2 (a) Top and (b) bottom surface resistivity of 8 vol% and 14 vol% Ni/PVC films as a function of film thickness

Compared with the top surface, the bottom surface resistivity was much lower and the trend of electric resistivity curve is quite different. As can be seen in Fig. 2(b), with increasing thickness from 0.17 mm to 0.25 mm, 0.32 mm and 0.38 mm of 8 vol% Ni/PVC films, the bottom surface resistivity decreases sharply from 76.7 Ω/square to 54.1 Ω/square, 32.5 Ω/square and 10.8 Ω/square, respectively; and then it decreased slightly when the thickness was higher than 0.38 mm. For 14 vol% Ni/PVC films, the bottom surface resistivity decreased slowly from 8.2 Ω/square for 0.18 mm to 2.9 Ω/square for 0.32 mm, and finally reached 1.5 Ω/square for 0.43 mm. In addition, surface resistivity of 8 vol% Ni/PVC films is larger than that of 14 vol% Ni/PVC films. This is due to the increase in content of Ni particles, which provided electric and magnetic dipoles in PVC matrix.

Generally, the electrical conductivity property for a conductive filler/polymer film is mainly dependent on the dispersion of conductive filler and the ease of formation of continuous conductive networks in polymer matrix[25]. It was worth mentioning that this asymmetric phenomenon of surface resistivity can be attributed to the special film structure.

As discussed before, Ni particles sink to the lower part of film due to gravity sedimentation, resulting in less Ni particles dispersed in the upper part. This makes the top surface of the films is a resin-rich region. Ni particles were divided by the insulating PVC (c.f., Figs. 1a, 1b and 1c). A long sedimentation time was required to obtain the thick film, resulting in more Ni particles sedimentation. The “conductor faults” between adjacent Ni particles in the top surface increased with film thickness, leading to a decrease of surface electrical conductivity. So the top surface had extremely low electrical conductivity, almost like an insulator. On the other side, lots of Ni particles were close to each other in bottom surface with increasing film thickness (c.f., Figs. 1g, 1h and 1i), resulting in less conductor faults breaking the conductive route, and contact points between Ni particles increased exponentially. So more perfect conductive networks were easily created, which was in favor of the

improvement in conductivity. Thus the bottom surface behaved almost as a conductor, especially for the thick films. Consequently, surface resistivity increased for top surface and decreased for the bottom one with film thickness, also the top surface had lower conductive ability than the bottom surface.

As is known to all, the EMI SE depends on the electrical conductivity of the material. Materials with lower surface resistivity have higher SE[26]. It is worthy to mention that this unique electrical property of Ni/PVC films make them very good candidates for electromagnetic shielding applications.

EMI Shielding Performance

Generally, it is essential to maintain functionality and integrity of electronic devices by attenuating of EMI. The SE is the amount of attenuation of incident radiation by a shielding material and is expressed in dB. If the incident electromagnetic power is denoted by P_{inc} and transmitted power by P_{trans}, then the EMI SE of a material can be expressed as SE(dB) = 10 lg(P_{inc}/P_{trans})[27]. Each 10 dB increase in SE means that the transmitted electromagnetic power attenuates to 1/10 of the former transmitted power.

Figure 3 exhibits the SE curves of Ni/PVC films with various thicknesses as a function of frequency ranging from 60 MHz to 1.5 GHz. PVC is intrinsically electrical insulating and transparent to electromagnetic radiation. It is observed that the EMI SE is found to increase with addition of Ni particles. Hence it is clear that the major contribution to EMI shielding comes from the conductive Ni networks. The EMI SE thickness dependency of all the films shows almost similar trend (c.f., Figs. 3a and 3b). Both figures show that EMI SE increases remarkably with film thickness for both 8 vol% and 14 vol% Ni/PVC films throughout the testing frequency range. For example, with increasing 14 vol% Ni/PVC film thickness from 0.18 mm to 0.26 mm, 0.32 mm, 0.38 mm and 0.43 mm, the SE increases from 27.0 dB to 32.6 dB, 35.2 dB, 38.1 dB and 43.2 dB, respectively. From Figs. 3(a) and 3(b), it is apparent that 14 vol% Ni/PVC film always displays substantially higher EMI SE than 8 vol% Ni/PVC film for the same film thickness. For example, the EMI SE of 14 vol% and 8 vol% Ni/PVC films with thickness of 0.32 mm are 35.2 dB and 21.4 dB, respectively. This is because the EMI SE of a shielding material depends on mobile charge carriers and magnetic dipoles. With increasing in Ni particles content, quantities of mobile charge carriers and magnetic dipoles increase in the system, leading to more impedance mismatch and hence more EMI SE[28]. Compared with 14 vol% Ni/PVC films, a large film thickness for 8 vol% Ni/PVC films was required to achieve the same SE. For a shielding level of 27 dB, the thickness of 8 vol% Ni/PVC film is more than two times to that of 14 vol% Ni/PVC film. It is well know that the target value of the EMI SE needed for commercial applications is about 20 dB[29] (*i.e.*, equal to 1% transmission of the electromagnetic power). Moreover, a SE of 30 dB, corresponding to 99.9% attenuation of the EMI radiation, is generally considered an adequate level of EMI shielding for many applications[6]. The above results indicate that most of Ni/PVC films in this study can meet the commercial application demands.

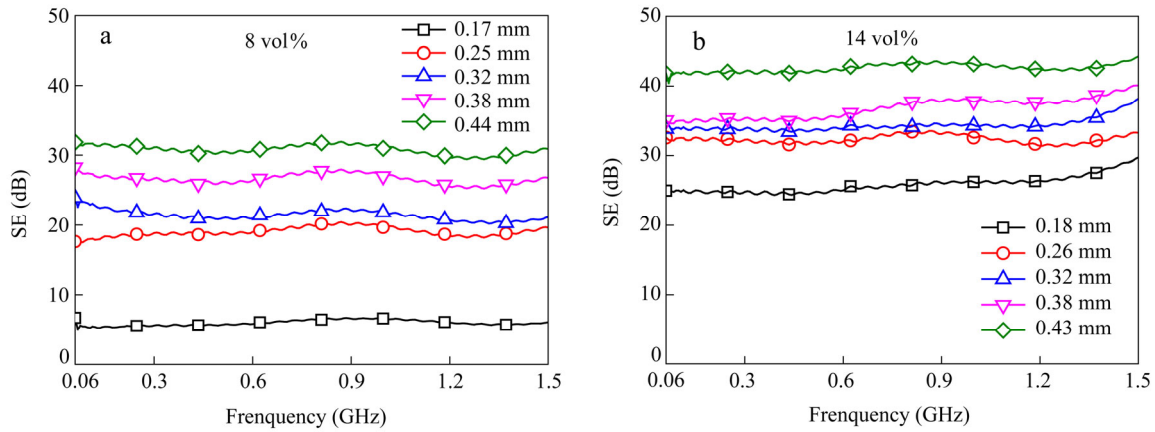

Fig. 3 EMI SE of (a) 8 vol% and (b) 14 vol% Ni/PVC films with various thicknesses as a function of frequency

A careful examination of SE results, as shown in Fig. 3, reveals that EMI SE of all films shows a slight wave-like variation against frequency. The variation of EMI SE against frequency is nonlinear and irregular, which indicates SE of the materials fluctuates with frequency of incident ray. This may be due to the irregular nature of the conductive network formed in PVC matrix[30].

As seen in Fig. 3, the films exhibit EMI SE of 7–43 dB at 1 GHz dependent on Ni content and film thickness. For films with the same Ni content, in consideration of the main contribution from the thickness on EMI SE, we try to build the relationship between EMI SE and film thickness. Figure 4 shows the effect of Ni/PVC film thickness on EMI SE at the fix frequency of 1.0 GHz. A nearly linear relationship can be found in this study. To explain the observed results, we propose the relationship between EMI SE and film thickness can be given by a straight line in Eq. (1):

$$Y = A \times X + B \tag{1}$$

where Y is the EMI SE at the corresponding thickness X, and A is a constant which represents the slope of the straight line. The slope value and correlation factor are listed in Table 1. A good fit was achieved between the experimental SE values and the fit function, with a correlation factor of 91% and 97% for 8 vol% and 14 vol% Ni/PVC films, respectively.

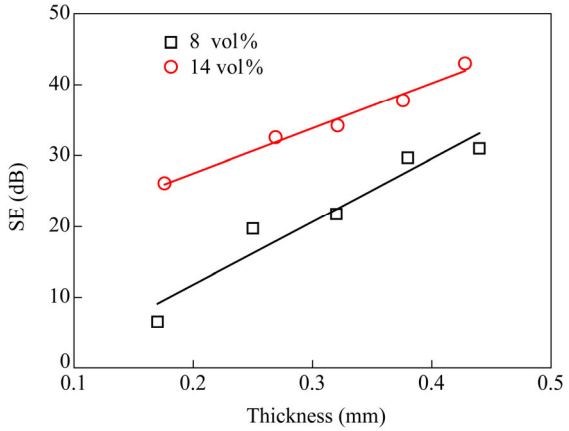

Fig. 4 EMI SE of 8 vol% and 14 vol% Ni/PVC films as a function of film thickness at a frequency of 1.0 GHz

Table 1. Slope value of 8 vol% and 14 vol% Ni/PVC films

Film	Slope value (dB/mm)	Correlation factor
8 vol% Ni/PVC	88.96	0.91
14 vol% Ni/PVC	63.57	0.97

The increased film thickness resulting in increasing SE means that the conductive networks interacting with the electromagnetic waves increase in this system[31]. As stated earlier, a long sedimentation time tends to increase the number of conductive networks in the film and also makes these conductive networks and electron tunnels become perfect. The conductive networks present in the lower part of the film act as conductive mesh which provides barriers to incident electromagnetic radiation[32]. With increase of film thickness, the number of such conducting networks (mesh) increases in the path of electromagnetic radiation. Thus, the mesh size decreases[33]. Therefore, the radiations those are not intercepted by thin films could be intercepted partly by thick films. So the electromagnetic SE improves monotonically with film thickness. This leads to better shielding performance of a thick shielding film.

In the present system, the slope, which is the measure of increase rate in EMI SE with respect to thickness, has found to be higher for 8 vol% Ni/PVC film than that of 14 vol% Ni/PVC film. This is in good agreement with their difference in bottom surface resistivity, where 8 vol% Ni/PVC film exhibits higher decreasing rate in

bottom surface resistivity than 14 vol% Ni/PVC film. The system which has the higher decreasing rate in bottom surface resistivity shows the faster increasing rate of EMI SE with film thickness.

In addition, good shielding performance even for such a thin film (less than 0.5 mm scale) provides additional advantages in terms of ease of processability, flexibility and cost effectiveness. It won't take up too much space in electronic devices for it is slim. Thus these properties make it an ideal candidate to reduce the size of complex electric equipments.

Pendulum Impact Resistance

As for pendulum impact resistance of a plastic film, the impact energy in joules is adopted to judge whether the film's character is ductile or brittle according to ASTM D3420-08a. Figure 5 shows the pendulum impact resistance of Ni/PVC films. Here, during the testing procedure, the hemispherical impact head penetrated the center of a film in the direction from top surface to bottom surface is termed as the forward impact, whereas the test in the opposite direction is defined as reverse impact. It would be observed that impact energy of both forward and reverse impact was significantly improved by increasing the film thickness. This is because the thicker film could absorb more energy during the fracture process. Interestingly, a detailed observation suggested that the energy absorbsion for forward impact was lower than that of the reverse impact. For example, the impact energy of forward and reverse impact was 2.26 J and 2.48 J for 8 vol% Ni/PVC film with the thickness of 0.32 mm. We speculated this discrepancy is attributed to the film asymmetry structure. Energy lost per unit of thickness (the impact absorbed energy divided by film thickness), as employed by some uniform film[34], doesn't offer much comparison for this study. Compared with the top surface, there was more Ni particles agglomeration in the bottom surface (c.f. Fig. 1). In addition, there is a weak interfacial adhesion between Ni particles and PVC matrix due to the unmodified Ni particles. Thus, a region of stress concentration, which requires less energy to propagate a crack, was created in the bottom surface. When the impact head hit from the top surface to the bottom surface (forward impact), the agglomerated Ni particles will cause stress concentration and make film burst, which lead to a lower impact resistance. On the other hand, there was less Ni particles embedded in top surface. The continuous PVC resin phase could endure more impact energy due to plastic deformation. As for the reverse impact, the top surface does decrease the amount of energy (from the impact blow) available for initiating and propagating large rupture cracks. In other words, the specimen could absorb more impact energy to rupture. So the film exhibits the better impact resistance for the reverse impact.

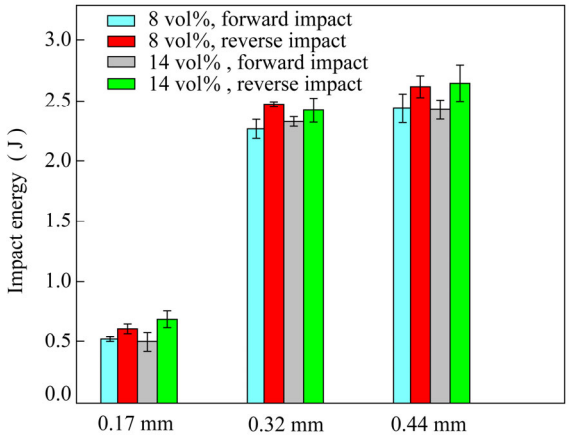

Fig. 5 Forward and reverse pendulum impact resistance of 8 vol% and 14 vol% Ni/PVC films with different film thickness

CONCLUSIONS

In conclusion, Ni/PVC films with asymmetric structure were successfully prepared *via* a controllable and cost-effective solution casting route. The concentration of Ni particles increased from top to bottom along the

thickness direction. This asymmetrical distribution of Ni particles played a critical role for implementation of special electrical conductivity and impact resistance performance. The bottom surface of the films behaved almost as a conductor, and the top surface just like an insulator. The top surface resistivity increased with film thickness, while the bottom surface one exhibited the different trend. In addition, the films exhibit better impact resistance for the reverse impact compared with the forward impact. An effective EMI shielding performance (over 40 dB) was achieved by this thin asymmetric film. This work may provide great opportunities and design rules for high-performance EMI shielding films in the future.

REFERENCES

1 Wang, H.Q., Zhang, H.Y., Zhao, W.F., Zhang, W. and Chen, G.H., Compos. Sci. Technol., 2008, 68(1): 238
2 Dhawan, S.K., Singh, K., Bakhshi, A.K. and Ohlan, A., Synthetic. Met., 2009, 159(21–22): 2259
3 Oh, Y., Chun, K.Y., Lee, E., Kim, Y.J. and Baik, S., J. Mater. Chem., 2010, 20(18): 3579
4 Kumar, R., Dhakate, S.R., Saini, P. and Mathur, R.B., RSC Adv., 2013, 3(13): 4145
5 Kwon, S., Ma, R., Kim, U., Choi, H.R. and Baik, S., Carbon, 2014, 68: 118
6 Yang, S.Y., Lozano, K., Lomeli, A., Foltz, H.D. and Jones, R., Composites Part A, 2005, 36(5): 691
7 Zhang, L., Wang, L.B., See, K.Y. and Ma, J., J. Mater. Sci., 2013, 48(21): 7757
8 Li, N., Huang, Y., Du, F., He, X.B., Lin, X., Gao, H.J., Ma, Y.F., Li, F.F., Chen, Y.S. and Eklund, P.C., Nano Lett., 2006, 6(6): 1141
9 Chen, Z., Xu, C., Ma, C., Ren, W. and Cheng, H.M., Adv. Mater., 2013, 25(9): 1296
10 Hu, M., Gao, J., Dong, Y., Li, K., Shan, G., Yang, S. and Li, R.K.Y., Langmuir, 2012, 28(18): 7101
11 Song, W.L., Cao, M.S., Lu, M.M., Bi, S., Wang, C.Y., Liu, J., Yuan, J. and Fan, L.Z., Carbon, 2014, 66: 67
12 Zhou, H., Wang, J., Zhuang, J. and Liu, Q., Rsc Adv., 2013, 3(45): 23715
13 Hu, L.B., Hecht, D.S. and Gruner, G., Chem. Rev., 2010, 110(10): 5790
14 Wu, H., Gu, A., Liang, G. and Yuan, L., J. Mater. Chem., 2011, 21(38): 14838
15 Chung, T.S., Jiang, L.Y., Li, Y. and Kulprathipanja, S., Prog. Polym. Sci., 2007, 32(4): 483
16 Hung, W.S., De Guzman, M., Huang, S.H., Lee, K.R., Jean, Y.C. and Lai, J.Y., Macromolecules, 2010, 43(14): 6127
17 Peng, N., Widjojo, N., Sukitpaneenit, P., Teoh, M.M., Lipscomb, G.G., Chung, T.S. and Lai, J.Y., Prog. Polym. Sci., 2012, 37(10): 1401
18 Jang, J. and Han, S., Composites Part A, 1999, 30(9): 1045
19 Fan, Z., Yan, J., Wei, T., Zhi, L., Ning, G., Li, T. and Wei, F., Adv. Funct. Mater., 2011, 21(12): 2366
20 Wang, B., Qin, D., Liang, G., Gu, A., Liu, L. and Yuan, L., J. Phys. Chem. C, 2013, 117(30): 15487
21 Luo, W., Yao, H.M., Yang, P.H. and Chen, C.S., J. Am. Ceram. Soc., 2009, 92(11): 2682
22 Song, Y.H., Pan, Y., Zheng, Q. and Yi, X.S., J. Polym. Sci., Part B: Polym. Phys., 2000, 38(13): 1756
23 Billas, I.M., Chatelain, A. and de Heer, W.A., Science, 1994, 265(5179): 1682
24 Chung, D.D.L., Carbon, 2001, 39(2): 279
25 Lu, J.X., Moon, K.S., Xu, J.W. and Wong, C.P., J. Mater. Chem., 2006, 16(16): 1543
26 Yuen, S.M., Ma, C.C. M., Chuang, C.Y., Yu, K.C., Wu, S.Y., Yang, C.C. and Wei, M.H., Compos. Sci. Technol., 2008, 68(3–4): 963
27 Colaneri, N.F. and Schacklette, L.W., IEEE T. Instrum. Meas., 1992, 41(2): 291
28 Singh, B.P., Saini, K., Choudhary, V., Teotia, S., Pande, S., Saini, P. and Mathur, R.B., J. Nanopart. Res., 2013, 16(1): 1
29 Al-Saleh, M.H. and Sundararaj, U., Carbon, 2009, 47(7): 1738
30 Rahaman, M., Chaki, T.K. and Khastgir, D., J. Mater. Sci., 2011, 46(11): 3989
31 Basavaraja, C., Kim, W.J., Kim, Y.D. and Huh, D.S., Mater. Lett., 2011, 65(19–20): 3120
32 Nayak, L., Khastgir, D. and Chaki, T.K., J. Mater. Sci., 2013, 48(4): 1492
33 Rahaman, M., Chaki, T.K. and Khastgir, D., Polym. Compos., 2011, 32(11): 1790
34 Barany, T., Izer, A. and Karger-Kocsis, J., Polym. Test., 2009, 28(2): 176